

1 **Methionine oxidation under anaerobic conditions in *Escherichia coli*.**

2

3 Laurent Loiseau¹, Alexandra Vergnes¹, Benjamin Ezraty¹ *

4

5 ¹ Aix-Marseille University, CNRS, Laboratoire de Chimie Bactérienne, Institut de Microbiologie de la
6 Méditerranée, Marseille, France.

7

8 * Corresponding author: ezraty@imm.cnrs.fr

9

10

For Peer Review

11 **ABSTRACT**

12 Repairing oxidative-targeted macromolecules is a central mechanism necessary for living
13 organisms to adapt to oxidative stress. Reactive oxygen and chlorine species preferentially
14 oxidize sulfur-containing amino acids in proteins. Among these amino acids, methionine
15 can be converted into methionine sulfoxide. This post-translational oxidation can be
16 reversed by methionine sulfoxide reductases, Msr enzymes. In Gram-negative bacteria, the
17 antioxidant MsrPQ system is involved in the repair of periplasmic oxidized-proteins.
18 Surprisingly, in this study we observed in *Escherichia coli* that *msrPQ* was highly expressed
19 in the absence of oxygen. We have demonstrated that the anaerobic induction of *msrPQ*
20 was due to chlorate (ClO_3^-) contamination of the Casamino Acids. Molecular investigation
21 led us to determine that the reduction of chlorate to the toxic oxidizing agent chlorite
22 (ClO_2^-) by the three nitrate reductases (NarA, NarZ and Nap) led to methionine oxidation of
23 periplasmic proteins. In response to this stress the *E. coli* HprSR two-component system
24 was activated, leading to over-production of MsrPQ. This study therefore supports the idea
25 that methionine oxidation in proteins is part of chlorate toxicity, and that MsrPQ can be
26 considered as an anti-chlorate/chlorite defense system in bacteria. Finally, this study
27 challenges the traditional view on the absence of Met-oxidation during anaerobiosis.

28

29 INTRODUCTION

30 Bacteria must effectively counter a myriad of stresses to survive (Fang *et al.*, 2016),
31 oxidative stress being one of the most challenging (Imlay, 2015). Under aerobic conditions
32 oxygen is used as the terminal electron acceptor for aerobic respiration, during which
33 reactive oxygen species (ROS) are produced endogenously through the reaction between
34 O₂ and univalent electron donors, such as metals, flavin and quinol (Imlay, 2013). In
35 addition to ROS, a wide variety of reactive nitrogen species (RNS) and reactive chlorine
36 species (RCS) act as powerful oxidants (Winterbourn and Kettle, 2013). A huge number of
37 these types of oxidants are released in order to combat pathogens during the host immune
38 oxidative-burst response. ROS, RNS and RCS are toxic and damage biological
39 macromolecules (nucleic acids, proteins, lipids), ultimately becoming life threatening
40 (Imlay, 2015).

41 Living organisms have developed two strategies to protect themselves from oxidants: the
42 first one, pre-oxidation, consists in eliminating harmful oxidants and relies on ROS
43 scavenging enzymes such as superoxide dismutases (SOD) to remove toxic O₂⁻ and
44 catalases/peroxidases to prevent H₂O₂ accumulation (Imlay, 2013); the second, post-
45 oxidation, involves the repair of oxidative-targeted macromolecules (Vaughan, 1997;
46 Merdanovic *et al.*, 2011; Aussel and Ezraty, 2021).

47 Several amino acids can be targeted by oxidants leading to post-translational modifications
48 and protein misfolding (Schramm *et al.*, 2020). Under oxidative stress, sulfur-containing
49 methionine residues are particularly sensitive to oxidation leading to the formation of
50 methionine sulfoxide (Met-O) (Kim *et al.*, 2014; Ezraty *et al.*, 2017). Oxidation of Met into
51 Met-O is reversible because of specific enzymes found in most living organisms: the
52 methionine sulfoxide reductases (Msr) (Ezraty *et al.*, 2005; Boschi-Muller and Branlant,

53 2014). The main representatives of this oxidized-protein repair family are MsrA and MsrB,
54 which are complementary and ubiquitous enzymes present in all domains of life from
55 humans to bacteria (Ezraty *et al.*, 2005). In prokaryotic cells, MsrA and MsrB are generally
56 located in the cytoplasm with some rare exceptions: for example the extracytoplasmic
57 MsrAB of *Neisseria* or *Streptococcus* species (Skaar *et al.*, 2002; Lowther *et al.*, 2002; Saleh
58 *et al.*, 2013).

59 A recently characterized member from *Escherichia coli* is MsrP, an enzyme responsible for
60 protein-MetO reduction in the periplasm of most Gram-negative bacteria (Gennaris *et al.*,
61 2015). MsrP is a molybdoenzyme containing a molybdenum cofactor of the molybdopterin
62 type (Mo-MPT), characteristic of the sulfite oxidase family (Loschi *et al.*, 2004). This
63 reductase works with the haem-binding membrane-bound partner MsrQ, which transmits
64 reducing power (Gennaris *et al.*, 2015). We have previously shown that the cistron *hiuH* -
65 encoding a transthyretin-like periplasmic protein (Lee *et al.*, 2005)- and *msrPQ* genes
66 belong to the same operon (El Hajj *et al.*, 2022). The *hiuH-msrPQ* operon is induced by RCS
67 in a two-component system HprSR-dependent manner (El Hajj *et al.*, 2022).

68 An anaerobic lifestyle is not considered to produce ROS. However, many obligate
69 anaerobes actually have ROS scavenging enzymes (superoxide dismutases or reductases;
70 catalases/ peroxidases) and oxidative-damage repair systems (Sheng *et al.*, 2014; Imlay,
71 2019). Msr genes (*msrA* and *msrB*) are also present in anaerobic organisms (including
72 *Clostridium acetobutylicum* or *perfringens* and *Chlorobium tepidum*) (Delaye *et al.*, 2007).
73 The presence of antioxidant mechanisms in anaerobes has been suggested to be required
74 following transient exposure to oxygen (Fu *et al.*, 2015).

75 In this study, we highlight the importance of the antioxidant enzyme MsrP in the absence
76 of oxygen for the facultative anaerobic bacterium *E. coli*. We observed periplasmic protein-
77 bound Met-O appearance during anaerobiosis following chlorate reduction to chlorite by

78 nitrate reductases. Mechanistically we have shown that MsrPQ production via HprSR
79 during chlorite stress is essential for *E. coli*. Finally, our results challenge the traditional
80 view that Met-oxidation is absent during anaerobiosis.

81

82 **RESULTS**

83 *msrP* expression is induced under anaerobic conditions in the presence of Casamino Acids

84 As reported in previous studies, we found that reactive chlorine species (HOCl and *N*-
85 Chlorotaurine) induce the expression of the *hiuH-msrPQ* operon in *E. coli* (El Hajj *et al.*,
86 2022). These results corroborate the idea that the oxidized-protein repair system is
87 necessary during oxidative stress. During this study, an unexpected observation was made:
88 this operon is also highly up-regulated under anaerobic conditions in the absence of any
89 apparent exogenous oxidative stress. This initial unpredicted observation suggested that
90 an antioxidant system might be needed in the absence of oxygen and was the subject of
91 subsequent studies. A more precise characterization of this effect led us to observe that the
92 induction of *hiuH-msrPQ* was present in both minimal and rich medium, but only in the
93 presence of Casamino Acids (CASA) (Fig. 1A). Indeed, by using a strain carrying the
94 chromosomal *hiuH-lacZ* translational fusion, we showed that under anaerobic conditions
95 the activity of the fusion increased about 20-fold in the presence of CASA in both media
96 (Fig. 1A), whereas under aerobic conditions the expression of the fusion was not affected
97 by the presence of CASA. This effect was confirmed on analysing MsrP protein levels by
98 western blot (Fig. 1B). These observations led us to hypothesize that the HiuH and/or
99 MsrPQ system might be important for cell growth under anaerobic conditions in the
100 presence of CASA. To test this hypothesis, we plated the $\Delta hiuH-msrPQ$, *hiuH*⁻, $\Delta msrP$ and

101 $\Delta msrQ$ mutant strains onto LB-agar plates supplemented with CASA under anaerobic
102 conditions and observed that disruption of the *hiuH-msrPQ* operon led to a defect in colony
103 morphology (Fig. 1C). Moreover, we observed that disruption of the single *hiuH* gene had
104 no effect on colony morphology, whereas deletions of *msrP* or *msrQ* showed a severe
105 phenotype (Fig. 1C). Indeed, we observed that the $\Delta hiuH-msrPQ$, $\Delta msrP$ and $\Delta msrQ$ mutant
106 colonies tended to be smaller than wild type colonies. The shape was readily
107 distinguishable, as the colonies of the mutant strains were cauliflower- or donut-shaped.
108 This morphological defect was not dependent on the density of the colonies on the plate
109 (Fig. S1) as previously described (Warne *et al.*, 1990). Overproduction of MsrP using the
110 plasmid pMsrP complemented only the $\Delta msrP$ mutant, whereas overproduction of MsrP
111 and MsrQ using the plasmid pMsrPQ was able to complement the mutant strains $\Delta hiuH-$
112 *msrPQ*, $\Delta msrP$ and $\Delta msrQ$ (Fig. 1D). These results support the conclusion that MsrPQ plays
113 an important role in bacterial growth under anaerobic conditions in the presence of CASA.

114

115 [FNR has an indirect effect on the regulation of *msrPQ* under anaerobic conditions in the](#)
116 [presence of CASA.](#)

117 We established that *msrPQ* was up-regulated under anaerobic conditions in the presence of
118 CASA and that the absence of the MsrPQ system rendered *E. coli* highly sensitive to these
119 conditions. However, it remained unclear why an antioxidant system appeared essential in
120 the absence of oxygen. An understanding of the regulatory pathway could clarify the
121 situation and therefore we initially investigated whether FNR, the master transcriptional
122 regulator of anaerobiosis (Spiro, 1994; Kiley and Beinert, 1998), was involved. We
123 examined *hiuH-lacZ* expression in a Δfnr strain: induction of the *hiuH-lacZ* fusion under

124 anaerobic conditions with CASA depended on the presence of FNR since no up-regulation
125 was observed in a Δfnr mutant (Fig. 2A). Furthermore, no accumulation of MsrP was
126 observed following immunoblotting of the Δfnr mutant under anaerobic conditions with
127 CASA (Fig. 2B). Interestingly, deletion of *fnr* was able to suppress the colony morphology
128 phenotype of the $\Delta msrP$ strain. The colonies of the $\Delta msrP \Delta fnr$ strain were smooth and
129 circular compared to the rough colonies of the wild-type strain (Fig. 2C). These results
130 suggest that FNR participates in *msrPQ* regulation. One prediction of our model is that FNR
131 directly binds and regulates the *hiuH-msrPQ* operon. To test this, we performed an *in silico*
132 analysis of the *hiuH-msrPQ* promoter region, using the DNA consensus binding site
133 previously determined (Myers *et al.*, 2013), and identified a putative FNR-binding site (5'-
134 **TTGAAGATAATCAA**-3') between positions -148bp and -162bp relative to the start codon
135 of the *hiuH* gene. We then constructed a deletion mutant of this putative FNR-binding site
136 in the *lacZ* fusion and showed that the deletion of this sequence had no impact on the
137 induction of the *hiuH-lacZ* fusion under anaerobic conditions with CASA (Fig. 2A). These
138 results favoured an indirect role for FNR in *msrPQ* regulation in *E. coli*.

139

140 [Nitrate reductases are required for the regulation of *msrPQ* under anaerobic conditions](#)
141 [with CASA.](#)

142 Molybdenum cofactor-dependent anaerobic respiration DMSO reductase family system
143 genes are FNR-regulated (Myers *et al.*, 2013). Deletion of the *mobAB* operon required for
144 the synthesis of the bis-Mo-MGD cofactor used by these systems, prevent accumulation of
145 MsrP under anaerobic conditions with CASA and suppressed the colony morphology
146 phenotype of the $\Delta msrP$ mutant strain, the colonies appeared smoother and less

147 segmented than wild-type colonies (Fig. 2B and C). This observation suggested that one or
148 more molybdenum cofactor-dependent anaerobic respiration systems are involved in this
149 phenotype. Indeed, the addition of alternative electron acceptors such as nitrate and TMAO
150 during anaerobic growth abrogated the effect of CASA on the induction of the *hiuH-lacZ*
151 fusion, while adding DMSO had no effect (Fig. 3A and B). Nitrate, and to a lesser extent
152 TMAO, chemically suppressed the $\Delta msrP$ colony morphology phenotype, while DMSO had
153 no impact (Fig. 3C). To perform anaerobic respiration using nitrate or TMAO as alternative
154 electron acceptors, *E. coli* relies on two cytoplasmic and one periplasmic nitrate reductase
155 (NR) (NarGHI, NarZYV and NapABC) (Fig. 4A) or TorAC respectively (Stewart, 1988;
156 Magalon and Mendel, 2015). Deletion of one NR had no effect on the induction of *msrPQ*
157 during anaerobiosis in the presence of CASA. However, the use of the $\Delta narG \Delta narZ \Delta napA$
158 mutant strain abrogated the up-regulation of *msrPQ*, suggesting that NR systems are
159 required for the induction of *msrPQ* during anaerobiosis in the presence of CASA (Fig. 4B).
160 Furthermore, no accumulation of MsrP was observed in the $\Delta narG \Delta narZ \Delta napA$ mutant
161 strain, whereas deleting either *narG*, *narZ*, *napA* had no effect on MsrP accumulation (Fig.
162 4C). We confirmed the involvement of the three NRs by deleting the two genes encoding
163 cytoplasmic nitrate uptake proteins (NarU and NarK) (Clegg *et al.*, 2002), and by showing
164 that the $\Delta narU \Delta narK \Delta napA$ mutant strain abrogated the up regulation of *msrPQ* (Fig. 4B).
165 Given that TMAO could partially suppress the $\Delta msrP$ colony morphology phenotype on
166 CASA, we conducted an experiment using the $\Delta torA$ mutant strain. Deletion of *torA* had no
167 effect on MsrP accumulation and did not suppress the colony morphology phenotype of the
168 $\Delta msrP$ (Fig. 4C and D). Surprisingly, deletion of *narG* alone was able to suppress the colony
169 morphology phenotype of the $\Delta msrP$ strain. The $\Delta msrP \Delta narG$ colonies were larger and
170 more opaque than wild-type colonies (Fig. 4D). These results suggested that the

171 requirement for MsrPQ during anaerobiosis in the presence of CASA depends on NR
172 activities.

173

174 [Reduction of chlorate to chlorite by nitrate reductases induces *msrPQ*.](#)

175 Given the multiple lines of evidence suggesting a link between MsrPQ and NRs during
176 anaerobiosis in the presence of CASA and in the absence of nitrate, we investigated
177 whether a component of the CASA could be used as a substrate for NRs. The 0.4 % CASA
178 solution was analysed by an external laboratory and a chlorate (ClO_3^-) contamination of
179 around 1.5 mg/L was detected. Chlorate, as an analogue of nitrate, is a substrate for NRs
180 which reduce chlorate to the toxic chlorite (ClO_2^-) (Glaser and DeMoss, 1971; Alefounder
181 and Ferguson, 1980; Giordano *et al.*, 1984). By analysing the expression of the *hiuH-lacZ*
182 fusion and the western blot, we confirmed that the addition of chlorate to the LB medium
183 under anaerobic conditions led to an increase in the expression of MsrP (Fig. 5A and B).
184 Moreover, the $\Delta\textit{msrP}$ strain showed a donut-shaped colony morphology phenotype on LB
185 plates containing chlorate (Fig. 5C), as observed with CASA. These results suggested that
186 the effects observed with CASA were due to the presence of chlorate in the CASA solution.
187 To confirm that the chlorate toxicity of the $\Delta\textit{msrP}$ strain comes from chlorate reduction to
188 chlorite by NRs, we attempted to suppress the phenotype of the $\Delta\textit{msrP}$ mutant by
189 overproducing chlorite dismutase (Cld) from *Dechloromonas aromatica* (Goblirsch *et al.*,
190 2010). The Cld enzyme catalyses the decomposition of chlorite into molecular oxygen and
191 chloride ions. Fig. 6A shows that Cld substantially suppressed the $\Delta\textit{msrP}$ mutant
192 phenotype. Next, we examined the effect of chlorite on the expression of the *hiuH-lacZ*
193 fusion. We observed that ClO_2^- induced the expression of the fusion in a dose-dependent

194 manner (Fig. 6B). Cld co-expression abrogated *hiuH-lacZ* up-regulation during ClO_2^- stress
195 (Fig. 6C and D). Overall, these results confirm that chlorite production via chlorate
196 reduction by NRs led to the ΔmsrP colony morphology phenotype and induction of *msrPQ*
197 expression.

198

199 [HprSR two-component system detects chlorite stress and induces *msrPQ*.](#)

200 We have previously demonstrated that HOCl induces the expression of *msrPQ* in an HprSR-
201 dependent manner (El Hajj *et al.*, 2022). HprSR is a two-component system in which HprS
202 and HprR are the sensor and the regulator respectively. We thus investigated the role of
203 HprSR in chlorite detection and performed immunodetection of MsrP from WT, ΔhprS and
204 ΔhprR strains cultivated anaerobically in the presence of chlorate. We observed an
205 accumulation of MsrP in the WT strain (Fig. 7), but no over-production of MsrP in the
206 ΔhprS and ΔhprR mutants (Fig. 7). These results indicate that the induction of the *hiuH-*
207 *msrPQ* operon by chlorate is dependent on the presence of a functional HprSR system and
208 suggest that HprS is able to sense chlorite production in the cell.

209

210 [Chlorite-damaged periplasmic proteins](#)

211 Having established that the periplasmic oxidized-protein repair system, MsrPQ, was over-
212 produced during chlorite stress, we sought to determine the effect of chlorite stress on the
213 methionine-redox state of periplasmic proteins by following the primary periplasmic
214 chaperone SurA, a specific substrate of MsrP in *E. coli* (Gennaris *et al.*, 2015). Using
215 western blots, we observed that SurA produced in a ΔmsrP mutant exposed to chlorite
216 treatment migrated more slowly than SurA produced in a WT strain or in a ΔmsrP mutant

217 that had not been exposed to chlorite (Fig. 8). This mobility-shift seen on SDS-PAGE was
218 evidence for methionine oxidation in SurA. These data suggest that chlorite was able to
219 oxidize Met residues *in vivo*. The findings presented so far suggest that periplasmic
220 proteins are oxidized by chlorite and that MsrP is important in the repair of chlorite-
221 induced protein damage.

222

223 Chlorate stress did not induce the expression of cytoplasmic methionine sulfoxide
224 reductases

225 We also examined whether chlorate stress induced the expression of the cytoplasmic
226 oxidized-protein repair genes, *msrA* and *msrB*. The strains carrying the chromosomal
227 reporter fusions *pmsrA-lacZ* and *pmsrB-lacZ* were cultured in the absence or in the
228 presence of chlorate under anaerobic conditions. No induction of *pmsrA-lacZ* and *pmsrB-*
229 *lacZ* fusions was observed during chlorate stress under anaerobic conditions (Fig. 9A).
230 Moreover, no colony morphology phenotype was observed using the $\Delta msrA \Delta msrB$ mutant
231 (Fig. 9B). Even the deletion of the *gshA* gene, that leads to decreased intracellular
232 glutathione levels (glutathione being putative quencher of cytoplasmic chlorite), had no
233 effect on colony morphology of the $\Delta msrA \Delta msrB$ mutant (i.e absence of donut/cauliflower-
234 shaped colonies) on LB-CASA under anaerobic conditions (Fig. S2). We conclude that
235 cytoplasmic methionine sulfoxide reductases are not up-regulated and that their absence
236 does not lead to morphological colony defects under chlorate stress.

237

238

239

240 **DISCUSSION**

241 Chlorate toxicity in bacteria has been studied for many decades, especially in relation to
242 anaerobic respiratory systems (Stewart, 1988). This study provides new insight into the
243 molecular mechanism of chlorate toxicity and has characterized, for the first time,
244 protection mechanisms against this stress in *E. coli*. We demonstrated that reduction of
245 chlorate to toxic chlorite leads to periplasmic protein oxidation. In response to this stress,
246 the *E. coli* HprSR two-component system is activated leading to the over-production of the
247 periplasmic oxidized-protein repair system, MsrPQ.

248

249 **A word of caution on chlorate contaminated Casamino Acids**

250 A fortuitous observation led us to discover that the Casamino Acids were contaminated
251 with chlorate, which represented the starting point for this study. This contamination does
252 not seem to be anecdotal since another global transcriptomic analysis study reported an
253 induction of *hiuH*, *yedY* and *yedZ* gene expression (as *msrP* and *msrQ* were previously
254 named) under anaerobic conditions (Covert *et al.*, 2004). CASA are a product of
255 hydrochloric acid hydrolysis of casein of animal origin and a dedicated study will be
256 necessary to investigate the presence of chlorate depending on the commercial origin of
257 the CASA. We would like to alert the wider population of CASA users to the possibility of
258 chlorite production during anaerobic experiments.

259

260 **New insight into chlorate reduction in *E. coli***

261 The ability of nitrate reductases to reduce chlorate was discovered in the sixties through
262 the isolation of chlorate-resistant (Chl^r) mutants and subsequent genetic studies (Glaser
263 and DeMoss, 1971; Alefounder and Ferguson, 1980; Giordano *et al.*, 1984). Retrospectively,
264 the analysis of this plethora of mutants has made it possible to identify all the steps from

265 gene expression to enzyme maturation involved in the activity of nitrate reductases. The
266 current model for chlorate reduction in *E. coli* is that chlorate is a substrate for the
267 cytoplasmic nitrate reductase A (NarA), but not for the second cytoplasmic reductase
268 (NarZ) or the periplasmic one (Nap). Moreover, it has been proposed that chlorate
269 transport into *E. coli* occurs independently of the nitrate transporters NarK and NarU
270 (Clegg *et al.*, 2002), however, these conclusions were made based on studies using high
271 chlorate concentrations (1 to 20 mM). Here, for the first time, we highlight an *E. coli*
272 chlorate phenotype at low chlorate concentrations (10 to 200 μ M), which allowed
273 reinvestigation of the chlorate reduction model. Our results showed that the three nitrate
274 reductases were able to reduce chlorate, as the concomitant deletion of the three nitrate
275 reductases was necessary to avoid chlorate induction of *msrP*. Moreover, given that the
276 $\Delta narU \Delta narK \Delta napA$ mutant phenocopy the $\Delta narG \Delta narZ \Delta napA$ mutant strain, we propose
277 that the nitrate transporters NarK and NarU are involved in chlorate import.

278

279 **New insight into chlorate/chlorite toxicity**

280 While chlorite production is known to be toxic to bacteria, the molecular mechanism
281 behind the toxicity of this oxidizing agent was unknown. Previous *in vitro* studies showed
282 that chlorite was able to oxidize protein-bound methionine (Melnik *et al.*, 2015). In this
283 study, we show that chlorite production by the anaerobic respiratory complex NRs
284 damages periplasmic proteins, such as the primary chaperone SurA. Moreover, we show
285 that chlorite activates the HprRS two-component system, whose activation has been
286 proposed to be mediated through a methionine redox switch located in the periplasmic
287 loop of the sensor (El Hajj *et al.*, 2022). Chlorite-HprRS activation leads to expression of the
288 periplasmic methionine sulfoxide reductase *msrPQ*. Together, these elements suggest that
289 protein methionine oxidation contributes to the molecular mechanisms of chlorate

290 toxicity. While the expression of cytoplasmic methionine sulfoxide reductases (*msrA* and
291 *msrB*) is not induced by chlorate treatment and that there is no pronounced morphological
292 defect in the $\Delta msrA \Delta msrB$ double mutant, the possibility that cytoplasmic proteins are
293 damaged by chlorite cannot be rule out, especially since NarA and NarZ have a
294 cytoplasmic-facing orientation, implying that chlorite is produced in the cytoplasm.
295 However, the fact that a strain lacking the periplasmic nitrate reductase, NapA, is still able
296 to activate *msrPQ* expression implies that cytoplasmic chlorite is, at least partially,
297 transferred to the periplasm, most likely driven by the membrane potential and the
298 nitrate/nitrite antiporter. Under high chlorate content, the rate of chlorite production
299 could be higher than the rate of periplasmic transfer, leading to oxidation of cytoplasmic
300 proteins and therefore MsrA/B could be important for chlorate resistance.

301

302 **MsrPQ appears as an anti-chlorite defense system**

303 The up-regulation of *msrPQ* during chlorate stress in *E. coli* is reminiscent of the response
304 found in the dissimilatory (per)chlorate-reducing bacteria (DPRB) which use (per)chlorate
305 as an electron acceptor (Wang and Coates, 2017). In the canonical perchlorate (ClO_4^-)
306 reduction pathway, perchlorate reductase (PcrAB) reduces ClO_4^- to chlorate (ClO_3^-) and
307 then to chlorite (ClO_2^-) in the periplasm. Chlorite dismutase (Cld) detoxifies chlorite by
308 generating chloride (Cl^-) and oxygen (O_2), and then a terminal oxygen reductase reduces
309 oxygen to water. In addition to the periplasmic anti-chlorite enzyme Cld, it has been shown
310 in the DPRB *Azospira suillum* that the *msrQP-mrpX* operon is induced during chlorite stress
311 via a sigma/anti-sigma factor system (SigF/NrsF). MrpX is a methionine-rich periplasmic
312 protein suggested to be an MsrP-dependent recyclable 'sponge' for oxidants (Melnyk *et al.*,
313 2015). Moreover, chlorate reduction in *Shewanella algae* ACDC has been shown to induce
314 the expression of *msrPQ* (Clark *et al.*, 2014). In this study, the *huiH-msrPQ* operon in *E. coli*

315 is not shown to be regulated by FNR, in accordance with previous studies which have not
316 reported *msrPQ* as direct FNR target genes (Myers *et al.*, 2013). Interestingly, in *Shewanella*
317 *oneidensis* the *msrPQ* operon has been suggested to be under the direct control of the FNR
318 homolog, EtrA (Zupok *et al.*, 2019), but to our knowledge this has not been experimentally
319 demonstrated. Therefore, it appears that different regulatory pathways (HprRS, SigF/NrsF,
320 FNR) are involved in adaptive regulation to chlorite, leading to the production of MsrPQ,
321 which can be considered as a necessary and efficient anti-chlorite defense system for
322 bacteria. The conservation of *msrPQ* (*yedYZ*) genes throughout Gram-negative bacteria
323 (Gennaris *et al.*, 2015) and more precisely in chlorate-respiring bacteria (Barnum *et al.*,
324 2018) illustrates the importance of having a periplasmic methionine sulfoxide reductase
325 system to overcome chlorite production.

326

327 **Methionine oxidation under anaerobic conditions**

328 This study reports for the first time a molecular explanation for the importance of
329 methionine sulfoxide reductases under physiological anaerobic conditions. This finding is
330 reminiscent of the study placing MsrA/B at the centre of the *Bacillus cereus* antioxidant
331 system under anaerobic fermentative conditions, however the molecular source of
332 methionine oxidation was not demonstrated (Duport *et al.*, 2021). Therefore, our study
333 shows that methionine redox control is not a phenomenon that is solely linked to a
334 reaction with reactive oxygen species.

335

336 Finally, these results become relevant if we assume that the natural life cycle of *E. coli* takes
337 place in the gastrointestinal tract and, most of its existence is spent under anaerobic
338 conditions. Chlorate contamination of drinking water could lead to the presence of chlorate

339 in the human gut and therefore put MsrPQ at the forefront of adaptive responses in
340 bacteria.

341

342

343 **ACKNOWLEDGEMENTS**

344

345 We thank the members of the Ezraty group for comments on the manuscript, advice and
346 discussion throughout the work. This work was supported by grants from the Agence
347 Nationale Recherche (#ANR-16-CE11-0012-02 METOXIC) and by the Prematuration
348 programme from the CNRS (#2021-22-Bachlosens).

349

350 The authors declare no conflict of interest.

351

352 **EXPERIMENTAL PROCEDURES**

353 **Chemical reagents and antibiotics**

354 All chemicals used were purchased from Sigma, Euromedex, or Fisher Scientific. CASA used
355 was purchased from Gibco™ Ref: #223050; batch n° 6266538. Sodium chlorate used was
356 purchased from Acros Organics Ref: #223222500. Antibiotics were used at the following
357 concentrations: Ampicillin (50 µg/ml) and kanamycin (25 µg/ml). Arabinose was used at
358 0.02%. Nitrate (40 mM), and trimethyl amine oxide (TMAO) (40 mM) were used as
359 electron acceptors.

360 **Strains and microbial techniques**

361 The strains used in this study are listed in Table 1. The *fnr::Kan^R*, *narG::Kan^R*, *narZ::Kan^R*,
362 *napA::Kan^R*, *narU::Kan^R*, *narK::Kan^R* and *torA::Kan^R* mutations from the BW25113 strain
363 (Keio library) (Baba *et al.*, 2006) were transduced into the MG1655 wild-type strain by P1
364 transduction standard procedure and checked by PCR. Strains were cured using pCP20
365 plasmid for successive transductions in order to obtain double and triple mutants. Primer
366 sequences used in this study are listed in Supplementary Table 2.

367 The *ΔhiuH-msrPQ* scarless mutant (strain LL996) was generated by lambda red
368 recombination adapted from Blank *et al.* (Blank *et al.*, 2011). Briefly, the DNA fragment was
369 amplified by PCR using primers 5-yedX-scarless and 3-wanner-msrQ (see Table 2) with
370 plasmid pWRG100 as a template. The resulting PCR product was electroporated into
371 BW25113 cells carrying pKD46 plasmid. After 1 h of expression, the cells were plated on
372 LB containing 25 µg/mL chloramphenicol. Selected colonies contained a *ΔhiuH-msrPQ sce-*
373 *I::cm* cassette which has been transduced in MG1655 cells harboring the pWRG99 plasmid.
374 The chloramphenicol cassette was then removed by counter selection using lambda red
375 recombination to insert a PCR product complementary to the flanking regions of the *sce-*
376 *I::cm* cassette on the chromosome. DsDNA is prepared from two complementary 96 mer
377 oligonucleotides generated with primers 5-scarlessyedXPQ and 3-scarlessyedXPQ. DsDNA
378 was then electroporated into MG1655 *ΔhiuH-msrPQ sce-I::cm* expressing lambda
379 recombinase from pWRG99, and after 1 hour expression serially diluted and plated on LB
380 containing 100 µg/mL ampicillin and 1 µg/mL anhydrotetracycline. pWRG99 also encoded
381 for the meganuclease I-Sce-I under the control of an anhydrotetracycline (aTc) inducible

382 promoter. The proper integration of the $\Delta hiuH$ -*msrPQ* was confirmed by diagnostic PCR
383 and sequenced.

384 The *hiuH* 3stop mutant (strain LL1913) was performed using the same method as
385 described above. Briefly, a $\Delta yedX$ *sce-I::cm* mutant was obtained by PCR using primers 5-
386 *yedX*-scarless and 3-*yedX*-scarless with plasmid pWRG100 as a template. The
387 chloramphenicol cassette was then removed by counter selection using lambda red
388 recombination to insert a *hiuH* 3stop PCR product amplified by PCR using primers
389 *yedX*_ATG_TAAx3_F and *yedX*_ATG_TAAx3_R.

390 The Δ FNR-putative-box::*cat*-*hiuH*-*lacZ* mutation was constructed in a one-step inactivation
391 by using lambda red recombination. A *cat* gene cassette was inserted into the putative FNR
392 box upstream *hiuH* gene. A DNA fragment containing the *cat* gene flanked with 5' and 3'
393 regions bordering the *E. coli* putative FNR box contained in the *hiuH*-*lacZ* construction was
394 amplified by PCR using pKD3 as a template and oligonucleotides 5del-wanner-*yedW* and
395 3del-wanner-*yedW*. PM1205 *hiuH*-*lacZ* strain, carrying the pKD46 plasmid, was
396 transformed by electroporation with the amplified fragment and Cm^r colonies were
397 selected.

398

399 Growth conditions

400 Cells were grown in Lysogeny Broth (LB) medium or in minimal medium (M9) supplied
401 with 0.2% glucose; for solid medium, 15 g/L of agar was supplemented. In aerobic
402 conditions, cells were grown in flask with a 1/10 volume of the flask capacity at 37 °C with
403 shaking at 150 rpm. In anaerobic conditions, cells were grown in 2 ml tubes full to the
404 brim, and for solid medium by using the GENbox Anaer generator (bioMérieux) in a
405 dedicated chamber.

406

407 CASA induction assays

408 The *hiuH*-*lacZ* -containing strain (CH184) was grown over night at 37 °C under aerobic or
409 anaerobic conditions in M9-glucose minimal medium or LB supplemented or not with
410 CASA (0.4% w/v). Levels of β -galactosidase were measured as previously described
411 (Miller, 1992). Growth under anaerobiosis was achieved by using 2 ml tubes full to the
412 brim.

413

414 Colony morphology assays

415 Strains were spread onto LB-agar plates containing CASA (0.4 % w/v) or NaClO₃ (16 µM).
416 The plates were incubated at 37 °C in anaerobic conditions for 48 hours. Growth under
417 anaerobiosis was achieved by using the GENbox Anaer generator (bioMérieux) in a
418 dedicated chamber. Ampicillin (50 µg/ml) and arabinose (0.02 %) were added to solid
419 media when required. The plates are then scanned using CanonScan 4200F and colony
420 morphology are observed using binocular magnifier Nikon SMZ800N. Colony shape
421 homogeneity was verified, and a representative colony was shown in the figure.

422

423 Chlorate detection in CASA solution

424 CASA solution (0.4 %) was analysed by Flandres-analyses laboratory (59180 Cappelle la
425 Grande) by liquid phase ion chromatography approach according to AFNOR NF EN ISO
426 10304-1 protocol.

427

428 Heterologous expression of the chlorite dismutase enzyme.

429 Genewiz from Azenta Life Sciences synthesized the pBAD24-clD-6His. The synthetic gene
430 was inserted into the *NcoI/Sall* sites of pBAD24 vector. This chimeric gene encode for a
431 protein composed by the 1-44 amino acids of the TAT signal sequence of MsrP of *E. coli*
432 and the 40-282 amino acids of chlorite dismutase of *Dechloromonas aromatica*. A His6-tag
433 at the *C terminus* of the polypeptide chain was introduced during the synthesis. 0.02 %
434 arabinose was used to induce the expression of *clD* gene. Immunoblot analysis using an
435 anti-His-tag antibody show the production of the non-mature form of Cld, suggesting that
436 the enzyme is not efficiently translocated the periplasm. However, this Cld form is able to
437 attenuate chlorite toxicity. MG1655 or CH184 strains harbouring pCld plasmid was grown
438 aerobically at 37 °C in LB supplemented with ampicillin (50 µg/ml) and arabinose (0.02%).
439 When cells reached an OD_{600nm} of 0.1, NaClO₂ (200 µM) was then added for 3.5 hours,
440 followed by β-galactosidase assays or immunoblot analysis using an anti-His-tag antibody.

441

442 Immunoblot analysis of MsrP production.

443 To assess MsrP production by CASA (0.04%) or chlorate (1, 10, 100 and 200 µM), cells
444 from overnight anaerobically cultures of the CH184, $\Delta hprR$ and $\Delta hprS$ strains were
445 harvested. The pellets were suspended in Laemmli buffer (2 % SDS, 10 % glycerol, 60 mM
446 Tris-HCl [pH 7.4], 0.01% bromophenol blue). The amount of protein loaded onto the gel
447 was standardized for each culture based on its A600 value. Samples were then heated for

448 10 min at 95 °C and loaded on SDS-PAGE. Immunoblot analysis was performed according
449 to standard procedures: the primary antibody was a guinea pig anti-MsrP antibody
450 (provided by Jean-François Collet Lab, De Duve Institute, Belgium). The secondary
451 antibody was an anti-guinea pig IgG conjugated to horseradish peroxidase (HRP)
452 (Promega). An ImageQuant LAS4000 camera (GE Healthcare Life Sciences) was used for
453 image chemiluminescence.

454

455 *In vivo* repair of oxidized SurA by MsrP.

456 MG1655 and $\Delta msrP$ strains were grown in LB at 37 °C in aerobic conditions. At OD_{600} of 0.1
457 cells were treated or not with $NaClO_2$ (200 μM). Cells were harvested after 2 hours of
458 $NaClO_2$ addition. The pellets were suspended in Laemmli buffer. The amount of protein
459 loaded onto the gel was standardized for each culture based on its A_{600} value. Samples
460 were then heated for 10 min at 95 °C and loaded on SDS-PAGE for immunoblot analysis
461 using anti-SurA antibody (provided by Jean-François Collet Lab, De Duve Institute,
462 Belgium).

463

464 **Table 1. Strains used in this study**

465 This table contains the information regarding the strains used in this study, including

466 strain names, genotypes, description and source.

467

Strain	Genotype and description	Source
MG1655	WT	Laboratory collection
BW25113	<i>lacI^q rrnB_{T14} ΔlacZ_{WJ16} hsdR514 ΔaraBAD_{AH33} ΔrhaBAD_{LD78}</i>	(Datsenko and Wanner, 2000)
PM1205	MG1655 <i>mal::lacI^q ΔaraBAD araC⁺ lacI':::P_{BAD}-cat-sacB-lacZ, mini λ tet^R</i>	(Mandin and Gottesman, 2009)
LL996	MG1655 <i>ΔhiuH-msrPQ</i>	This study
LL1913	MG1655 <i>hiuH</i> 3stop mutant	This study
BE107	MG1655 <i>ΔmsrP::Kan^r</i>	(Gennaris <i>et al.</i> , 2015)
CH380	MG1655 <i>ΔmsrP</i>	This study
BE206	MG1655 <i>ΔmsrQ::Kan^r</i>	This study
CH184	PM1205 <i>hiuH-lacZ</i>	(El Hajj <i>et al.</i> , 2022)
LL1103	PM1205 <i>hiuH-lacZ Δfnr::Kan^r</i>	This study
LL1699	PM1205 (<i>lacI-yedW::cat</i>)- <i>hiuH-lacZ</i> (deletion of the putative FNR box)	This study
LL216	MG1655 <i>Δfnr::Kan^r</i>	This study
TP1004	RK4353 <i>ΔmobAB::Kan^r</i>	Received from Tracy Palmer
LL1119	MG1655 <i>ΔmsrP Δfnr::Kan^r</i>	This study
LL1120	MG1655 <i>ΔmsrP ΔmobAB::Kan^r</i>	This study
LL1138	MG1655 <i>ΔnarG::Kan^r</i>	This study
LL1170	LL1138 (<i>lacI-yedW::cat</i>)- <i>hiuH-lacZ</i>	This study
LL1130	MG1655 <i>ΔnarZ::Kan^r</i>	This study
LL1168	CH184 <i>ΔnarZ::Kan^r</i>	This study
LL1129	MG1655 <i>ΔnapA::Kan^r</i>	This study
LL1166	CH184 <i>ΔnapA::Kan^r</i>	This study
LL1144	MG1655 <i>ΔnarG::Kan^r ΔnarZ ΔnapA</i>	This study
LL1171	LL1144 (<i>lacI-yedW::cat</i>)- <i>hiuH-lacZ</i>	This study

LL1169	MG1655 $\Delta narU \Delta narK::Kan^r$	This study
LL1231	LL1169 (<i>lacI-yedW::cat</i>)- <i>hiuH-lacZ</i>	This study
LL1187	MG1655 $\Delta napA \Delta narU \Delta narK::Kan^r$	This study
LL1232	LL1187 (<i>lacI-yedW::cat</i>)- <i>hiuH-lacZ</i>	This study
LL1146	MG1655 $\Delta msrP \Delta narZ::Kan^r$	This study
LL1147	MG1655 $\Delta msrP \Delta napA::Kan^r$	This study
LL1148	MG1655 $\Delta msrP \Delta narG::Kan^r$	This study
LL1145	MG1655 $\Delta torA::Kan^r$	This study
LL1153	MG1655 $\Delta msrP \Delta torA::Kan^r$	This study
BE152	MG1655 $\Delta msrA \Delta msrB$	(Henry <i>et al.</i> , 2021)
LL1296	MG1655 $\Delta msrA \Delta msrB \Delta gshA::Kan^r$	This study
JB56	IBPC5321 <i>msrA'</i> - <i>lacZ</i>	(Bos <i>et al.</i> , 2013)
JB44	IBPC5321 <i>msrB'</i> - <i>lacZ</i>	(Bos <i>et al.</i> , 2013)
BE255	MG1655 $\Delta hprR::Kan^r$	This study
BE254	MG1655 $\Delta hprS::Kan^r$	This study

468

469

470

471 **Table 2. Primers used in this study**

472 This table contains the information regarding the primers used in this study, including
 473 primer names and sequences.

474

Name	Sequence (5' to 3')
5-yedX-scarless	cgctatcctcaaaactcattcacatgacaaggatataaacgaccttacgccccgcctgc
3-wanner-msrQ	acatccggcaggataacgcgtactttgtcggcaatatgaagcatatgaatatcctcctta
5-scarlessyedXPQ	gcttttcgctatcctcaaaactcattcacatgacaaggatataaactcatattgccgacaaagtacgc ggtatccctgccggatgtggcgcgag
3-scarlessyedXPQ	ctcgcgccacatccggcaggataacgcgtactttgtcggcaatatgaagttatatccttgcatgtga atgagttttgaggatagcgaaaaagc
3- yedX-scarless	ccgtaacatctgattcttttaaaattgattcttttcatctagactatattaccctgtt
<i>yedX</i> _ATG_TAAx3_F	cgctatcctcaaaactcattcacatgacaaggatataaacatgtaataataatatttagtactctcgta gcaacg
<i>yedX</i> _ATG_TAAx3_R	ccctaacagtagcagatctgcttttacatatttatgcattaactgccacgataggtgaataccc
5del-wanner- <i>yedW</i>	cgaagcggcatgcatttacgttgacaccatcgaatggcgcgtgtaggctggagctgcttc
3del-wanner- <i>yedW</i>	ggctgtttctataacatattgattatggcatatttttccatatgaatatcctcctta

475

476

477

478 **Table 3. Plasmids used in this study**

479 This table contains the information regarding the plasmids used in this study, including
 480 plasmid names, genotypes, description and source.

481

Plasmid	Genotype and description	Source
pAG177 (p-empty)	pTAC-MAT-Tag-2-NdeI, Amp ^R	(Gennaris <i>et al.</i> , 2015)
pAG192 (pMsrP)	pTAC-MAT-Tag-2-NdeI MsrP, Amp ^R	(Gennaris <i>et al.</i> , 2015)
pAG195 (pMsrPQ)	pTAC-MAT-Tag-2-NdeI MsrP-MsrQ, Amp ^R	(Gennaris <i>et al.</i> , 2015)
pKD46	λ Red-expression under control of arabinose-inducible promoter, temperature-sensitive, Amp ^R	(Datsenko and Wanner, 2000)
pCP20	<i>FLP^t</i> , Φ cI857 ⁺ , Φ P _R Rep ^{ts} , Amp ^R , Cm ^R	(Cherepanov and Wackernagel, 1995)
pWRG99	pKD46 with I-SceI endonuclease under control of tetracycline-inducible promoter (<i>P_{tetA}</i>), temperature-sensitive, orientation 2 (5'→3': I-SceI- <i>tetR</i>), Amp ^R	(Blank <i>et al.</i> , 2011)
pWRG100	pKD3 with I-SceI recognition site, Cm ^R	(Blank <i>et al.</i> , 2011)
pBAD24	PBAD promoter, pACYC184-based, arabinose inducible, Amp ^R	Laboratory collection
<i>pBAD24-cld-6His</i>	pBAD24-NcoI/Sall containing <i>cld</i> gene from <i>Dechloromonas aromatic</i> , Amp ^R	Genewiz/Azenta Life Sciences

482

483

484

485 **LEGENDS**

486 **Figure 1. A central role for MsrPQ under anaerobic conditions in the presence of**
 487 **CASA.**

488 **A)** Evaluation of *hiuH-msrPQ* expression under aerobic and anaerobic conditions. The
 489 expression of the *hiuH-lacZ* fusion, in strain CH184, was used as a proxy for *msrPQ*
 490 expression. Strain CH184 was cultured overnight at 37°C in M9-Glucose or LB
 491 supplemented or not with 0.4 % CASA, under aerobic or anaerobic conditions, followed by
 492 β -galactosidase assays. Results are expressed as means +/- SD (n = 3). Asterisks indicate a
 493 statistically significant difference between the absence and the presence of CASA,
 494 ***P<0.001 (Ordinary one-way ANOVA with Tukey's multiple comparison test) **B)**
 495 Immunoblot analysis using an anti-MsrP antibody showing the production of MsrP under
 496 anaerobic conditions in the presence of 0.4 % CASA. The image is representative of
 497 experiments carried out in triplicate. **C)** Evaluation of colony morphology on LB-CASA agar
 498 plates. Wild-type (MG1655), Δ *hiuH-msrPQ* (LL996), *hiuH*⁻ (LL1913), Δ *msrP* (CH380) and
 499 Δ *msrQ* (BE206) strains were plated onto LB-agar containing 0.4 % CASA. The plates were
 500 incubated at 37 °C under anaerobic conditions for 48 hours. The plates were then scanned
 501 (left panel) and observed using a binocular magnifier (right panel). The images are
 502 representative of experiments carried out (at least) in triplicate. **D)** Colony morphology of
 503 Δ *hiuH-msrPQ* (LL996), Δ *msrP* (CH380) and Δ *msrQ* (BE206) strains carrying either an
 504 empty vector, pMsrP or pMsrQ plasmids. The strains were plated onto LB-ampicillin-agar
 505 containing 0.4 % CASA. The plates were incubated at 37 °C under anaerobic conditions for
 506 48 hours before being observed using a binocular magnifier. The images are
 507 representative of experiments carried out at least three times.

508

509 **Figure 2. An indirect role for FNR in *msrPQ* expression.**

510 **A)** Effect of *fnr* deletion on *hiuH-msrPQ* expression. Wild-type and Δ *fnr* strains carrying the
 511 *hiuH-lacZ* fusion and the wild-type strain carrying the p**hiuH-lacZ* fusion (deletion of the
 512 putative FNR box) were cultured overnight in LB supplemented with 0.4 % CASA under
 513 anaerobic conditions, followed by β -galactosidase assays. Results are expressed as means
 514 +/- SD (n = 3). Asterisks indicate a statistically significant difference between mutant and
 515 the WT, ***P<0.001 (Ordinary one-way ANOVA with Tukey's multiple comparison test) **B)**
 516 Immunoblot analysis using an anti-MsrP antibody, showing the production of MsrP from
 517 wild-type, Δ *msrP* (CH380), Δ *fnr* (LL216) and Δ *mobAB* (TP1004) strains cultivated under

518 anaerobic conditions in the presence of 0.4 % CASA. The image is representative of
519 experiments carried out in triplicate. **C)** Evaluation of colony morphology on LB-CASA agar
520 plates. Wild-type (MG1655), $\Delta msrP$ (CH380), $\Delta msrP \Delta fnr$ (LL1119) and $\Delta msrP \Delta mobAB$
521 (LL1120) strains were plated onto LB-CASA (0.4 %) agar and incubated at 37 °C under
522 anaerobic conditions for 48 hours before being scanned (upper part) and observed using a
523 binocular magnifier (lower panel). The images are representative of experiments carried
524 out at least three times.

525

526 **Figure 3. Nitrate chemically suppresses the effect of CASA on MsrP.**

527 **A)** Effect of the addition of alternative electron acceptors (nitrate, DMSO and TMAO) on
528 *hiuH-msrPQ* expression. Wild-type strain carrying the *hiuH-lacZ* fusion was cultured
529 overnight in LB supplemented with 0.4 % CASA in the presence of nitrate, DMSO or TMAO
530 (40 mM) under anaerobic conditions, followed by β -galactosidase assays. Results are
531 expressed as means +/- SD (n = 3). Asterisks indicate a statistically significant difference
532 between the absence and the presence of electron acceptors, **P<0.01 and ***P<0.001
533 (Ordinary one-way ANOVA with Tukey's multiple comparison test) **B)** Immunoblot
534 analysis using an anti-MsrP antibody showing the production of MsrP from wild-type
535 cultivated following the procedure described for panel (A). The image is representative of
536 experiments carried out in triplicate. **C)** Evaluation of colony morphology on LB-CASA agar
537 plates supplemented with alternative electron acceptors. The $\Delta msrP$ (CH380), strain was
538 plated onto LB-CASA (0.4 %) agar containing nitrate, DMSO or TMAO (40 mM). Plates were
539 incubated at 37 °C under anaerobic conditions for 48 hours before scanning. The images
540 are representative of experiments carried out at least three times.

541

542 **Figure 4. The three nitrate reductases are required for the regulation of *msrPQ***
543 **under anaerobic conditions with CASA.**

544 **A)** Schematic representation of the respiratory nitrate reductase systems in *E. coli*. The
545 cytoplasmic nitrate reductases NarA (in blue) and NarZ (in orange) composed of NarGHI
546 and NarZYV subunits respectively, are able to reduce nitrate (NO_3^-) to nitrite (NO_2^-) in the
547 cytoplasm. The periplasmic nitrate reductase NapA (in green) composed of NapABC
548 subunits, reduce NO_3^- in the periplasmic compartment. The nitrate importers NarU (in
549 yellow) and NarK (in purple) move nitrate into the cytoplasm. **B)** Effect of *nar* and *nap*
550 deletions on *hiuH-msrPQ* expression. Wild-type, $\Delta narG$ (LL1170), $\Delta narZ$ (1168), $\Delta napA$

551 (LL1166), $\Delta narG \Delta narZ \Delta napA$ (LL1171), $\Delta narU \Delta narK$ (LL1231) and $\Delta narU \Delta narK \Delta napA$
552 (LL1232) strains carrying the *hiuH-lacZ* fusion were cultured overnight in LB
553 supplemented with 0.4 % CASA under anaerobic conditions, followed by β -galactosidase
554 assays. Results are expressed as means \pm SD (n = 3). Asterisks indicate a statistically
555 significant difference between mutants and the WT, $***P < 0.001$ and ns, not significant
556 (Ordinary one-way ANOVA with Tukey's multiple comparison test). **C)** Immunoblot
557 analysis using an anti-MsrP antibody showing the production of MsrP from strains
558 indicated below the panel, cultivated following the same procedure as in panel (B). The
559 image is representative of experiments carried out in triplicate. **D)** Evaluation of colony
560 morphology on LB-CASA agar. Wild type (MG16555), $\Delta msrP$ (CH380), $\Delta msrP \Delta narG$
561 (LL1148), $\Delta msrP \Delta narZ$ (LL1146), $\Delta msrP \Delta napA$ (LL1147) and $\Delta msrP \Delta torA$ (LL1153)
562 strains were plated onto LB-CASA (0.4 %) agar. The plates were incubated at 37 °C under
563 anaerobic conditions for 48 hours before being scanned (upper panel) and observed using
564 a binocular magnifier (lower panel). The images are representative of experiments carried
565 out at least three times.

566

567 **Figure 5. Chlorate (ClO_3^-) contaminated CASA.**

568 **A)** Effect of chlorate on *hiuH-msrPQ* expression under anaerobic conditions. The
569 expression of the *hiuH-lacZ* fusion in strain CH184 was used as a proxy for *msrPQ*
570 expression. Strain CH184 was cultured overnight at 37 °C in LB supplemented or not with
571 $NaClO_3$ (10 μM), under anaerobic conditions, followed by β -galactosidase assays. Results
572 are expressed as means \pm SD (n = 3). Asterisks indicate a statistically significant
573 difference between the absence and the presence of $NaClO_3$, $***P < 0.001$ (Ordinary one-
574 way ANOVA with Tukey's multiple comparison test). **B)** Immunoblot analysis using an
575 anti-MsrP antibody showing the production of MsrP from the wild-type strain cultivated
576 overnight at 37 °C in LB supplemented with $NaClO_3$ (1 to 100 μM) under anaerobic
577 conditions. The image is representative of experiments carried out in triplicate. **C)** The
578 wild type (MG16555) strain was plated onto LB-agarose supplemented or not with $NaClO_3$
579 (16 μM). The plates were incubated at 37 °C under anaerobic conditions for 48 hours
580 before being observed using a binocular magnifier. The images are representative of
581 experiments carried out at least three times.

582

583 **Figure 6. Effect of the heterologous expression of chlorite dismutase.**

584 **A)** Chlorite dismutase (Cld) from *Dechloromonas aromatica* was expressed using the pCld
585 plasmid. The $\Delta msrP$ strain carrying the empty vector (pBad24) or pCld was spread onto
586 LB-agar plates supplemented or not with NaClO_3 (16 μM), containing ampicillin and
587 arabinose (0.02 %). The plates were incubated at 37 °C under anaerobic conditions for 48
588 hours before being observed using a binocular magnifier. The images are representative of
589 experiments carried out at least three times. **B)** Effect of chlorite (ClO_2^-) on *hiuH-msrPQ*
590 expression under aerobic conditions. The expression of the *hiuH-lacZ* fusion in strain
591 CH184 was used as a proxy for *msrPQ* expression. Strain CH184 was cultured at 37°C in LB
592 to $\text{OD}_{600} \approx 1.5$ under aerobic conditions, NaClO_2 (20 or 200 μM) was then added and β -
593 galactosidase assays were conducted at different time points for each condition. **C)** Effect
594 of the production of Cld on *hiuH-lacZ* fusion during chlorite stress. The CH184 strain
595 carrying empty vector (pBad24) or pCld was cultured at 37°C in LB (supplemented with
596 ampicillin and arabinose 0.02 %) to $\text{OD}_{600} \approx 0.1$ under aerobic conditions. NaClO_2 (200 μM)
597 was then added for 3.5 hours, followed by β -galactosidase assays. Results are expressed as
598 means \pm SD (n = 3). Asterisks indicate a statistically significant difference between the
599 absence and the presence of Cld, *** $P < 0.001$ (Ordinary one-way ANOVA with Tukey's
600 multiple comparison test). **D)** Immunoblot analysis using an anti-MsrP antibody, showing
601 the production of MsrP from the strains indicated above the panel, cultivated following the
602 same procedure as described for panel (C).

603
604 **Figure 7. Chlorate regulates *msrPQ* expression in an HprSR-dependent manner.**

605 Immunoblot analysis using an anti-MsrP antibody showing the production of MsrP from
606 wild-type (MG1655), $\Delta hprR$ (BE255) and $\Delta hprS$ (BE254) strains cultivated overnight at 37
607 °C in LB supplemented with NaClO_3 (20 μM) under anaerobic conditions. The image is
608 representative of experiments carried out in triplicate.

609
610 **Figure 8. MsrP repairs the chlorite-oxidized SurA.**

611 Wild type and $\Delta msrP$ cells were grown in LB at 37°C under aerobic conditions. At an OD_{600}
612 of 0.1 cells were treated or not with NaClO_2 (200 μM) for 2 hours and the SurA protein was
613 analysed by immunoblotting. In the $\Delta msrP$ strain, chlorite treatment led to the appearance
614 of the oxidized form of SurA (SurAox) which exhibits a mobility shift on SDS-PAGE
615 resulting from Met-O formation. This blot is representative of three independent
616 experiments.

617

618 **Figure 9. Cytoplasmic methionine sulfoxide reductases are not induced by chlorate.**

619 **A)** Effect of chlorate on *msrA* and *msrB* expression under anaerobic conditions. The strains
620 JB56 and JB44, harbouring the *pmsrA-lacZ* and *pmsrB-lacZ* fusions respectively, were
621 cultured overnight at 37°C in LB supplemented or not with NaClO₃ (10 µM), under
622 anaerobic conditions, followed by β-galactosidase assays. The *hiuH-lacZ* fusion (CH184)
623 was used as a control. Results are expressed as means +/- SD (n = 3). Asterisks indicate a
624 statistically significant difference between the absence and the presence of NaClO₃,
625 ***P<0.001 and ns, not significant (Ordinary one-way ANOVA with Tukey's multiple
626 comparison test). B) Colony morphology of Δ *msrP* (CH380) and Δ *msrA* Δ *msrB* (BE152)
627 strains. The strains were plated onto LB-CASA (0.4 %) agar and incubated at 37 °C under
628 anaerobic conditions for 48 hours. The plates were then scanned (upper panel) and
629 observed using a binocular magnifier (lower panel). The images are representative of
630 experiments carried out at least three times.

631

632 **REFERENCES**

633

634 Alefounder, P.R., and Ferguson, S.J. (1980) The location of dissimilatory nitrite reductase
635 and the control of dissimilatory nitrate reductase by oxygen in *Paracoccus denitrificans*.
636 *Biochem J* **192**: 231–240.

637

638 Aussel, L., and Ezraty, B. (2021) Methionine Redox Homeostasis in Protein Quality Control.
639 *Front Mol Biosci* **8**: 1–8.

640

641 Baba, T., Ara, T., Hasegawa, M., Takai, Y., Okumura, Y., Baba, M., *et al.* (2006) Construction of
642 *Escherichia coli* K-12 in-frame, single-gene knockout mutants: The Keio collection. *Mol Syst*
643 *Biol* **2**.

644

645 Barnum, T.P., Figueroa, I.A., Carlström, C.I., Lucas, L.N., Engelbrektson, A.L., and Coates, J.D.
646 (2018) Genome-resolved metagenomics identifies genetic mobility, metabolic interactions,
647 and unexpected diversity in perchlorate-reducing communities. *ISME J* **12**: 1568–1581
648 <http://www.nature.com/articles/s41396-018-0081-5>.

649

650 Blank, K., Hensel, M., and Gerlach, R.G. (2011) Rapid and Highly Efficient Method for
651 Scarless Mutagenesis within the *Salmonella enterica* Chromosome. *PLoS One* **6**: e15763.

652

653 Bos, J., Duverger, Y., Thouvenot, B., Chiaruttini, C., Branlant, C., Springer, M., *et al.* (2013)
654 The sRNA RyhB Regulates the Synthesis of the *Escherichia coli* Methionine Sulfoxide
655 Reductase MsrB but Not MsrA. *PLoS One* **8**.

656

657 Boschi-Muller, S., and Branlant, G. (2014) Methionine sulfoxide reductase: Chemistry,
658 substrate binding, recycling process and oxidase activity. *Bioorg Chem* **57**: 222–230.

659

660 Cherepanov, P.P., and Wackernagel, W. (1995) Gene disruption in *Escherichia coli*: TcR and
661 KmR cassettes with the option of Flp-catalyzed excision of the antibiotic-resistance
662 determinant. *Gene* **158**: 9–14.

663

664 Clark, I.C., Melnyk, R.A., Iavarone, A.T., Novichkov, P.S., and Coates, J.D. (2014) Chlorate

- 665 reduction in *Shewanella algae* ACDC is a recently acquired metabolism characterized by
666 gene loss, suboptimal regulation and oxidative stress. *Mol Microbiol* **94**: 107–125.
667
- 668 Clegg, S., Yu, F., Griffiths, L., and Cole, J.A. (2002) The roles of the polytopic membrane
669 proteins NarK, NarU and NirC in Escherichia coli K-12: two nitrate and three nitrite
670 transporters. *Mol Microbiol* **44**: 143–155.
671
- 672 Covert, M.W., Knight, E.M., Reed, J.L., Herrgard, M.J., and Palsson, B.O. (2004) Integrating
673 high-throughput and computational data elucidates bacterial networks. *Nature* **429**: 92–
674 96.
675
- 676 Datsenko, K.A., and Wanner, B.L. (2000) One-step inactivation of chromosomal genes in
677 Escherichia coli K-12 using PCR products. *Proc Natl Acad Sci U S A* **97**: 6640–5
678 [http://www.pubmedcentral.nih.gov/articlerender.fcgi?artid=18686&tool=pmcentrez&ren](http://www.pubmedcentral.nih.gov/articlerender.fcgi?artid=18686&tool=pmcentrez&rendertype=abstract)
679 [dertype=abstract](http://www.pubmedcentral.nih.gov/articlerender.fcgi?artid=18686&tool=pmcentrez&rendertype=abstract).
680
- 681 Delaye, L., Becerra, A., Orgel, L., and Lazcano, A. (2007) Molecular Evolution of Peptide
682 Methionine Sulfoxide Reductases (MsrA and MsrB): On the Early Development of a
683 Mechanism That Protects Against Oxidative Damage. *J Mol Evol* **64**: 15–32.
684
- 685 Duport, C., Madeira, J.-P., Farjad, M., Alpha-Bazin, B., and Armengaud, J. (2021) Methionine
686 Sulfoxide Reductases Contribute to Anaerobic Fermentative Metabolism in *Bacillus cereus*.
687 *Antioxidants* **10**: 819.
688
- 689 Ezraty, B., Aussel, L., and Barras, F. (2005) Methionine sulfoxide reductases in prokaryotes.
690 *Biochim Biophys Acta* **1703**: 221–9 <http://www.ncbi.nlm.nih.gov/pubmed/15680230>.
691
- 692 Ezraty, B., Gennaris, A., Barras, F., and Collet, J.-F. (2017) Oxidative stress, protein damage
693 and repair in bacteria. *Nat Rev Microbiol* **15**: 385–396
694 <http://www.nature.com/doifinder/10.1038/nrmicro.2017.26>.
695
- 696 Fang, F.C., Frawley, E.R., Tapscott, T., and Vázquez-Torres, A. (2016) Bacterial Stress
697 Responses during Host Infection. *Cell Host Microbe* **20**: 133–143.

- 698 Fu, H., Yuan, J., and Gao, H. (2015) Microbial oxidative stress response: Novel insights from
699 environmental facultative anaerobic bacteria. *Arch Biochem Biophys* **584**: 28–35.
700
- 701 Gennaris, A., Ezraty, B., Henry, C., Agrebi, R., Vergnes, A., Oheix, E., *et al.* (2015) Repairing
702 oxidized proteins in the bacterial envelope using respiratory chain electrons. *Nature* **528**:
703 409–412
704 <http://www.nature.com/doi/10.1038/nature15764>
705 <http://www.ncbi.nlm.nih.gov/pubmed/26641313>.
706
- 707 Giordano, G., Violet, M., Medani, C., and Pommier, J. (1984) A common pathway for the
708 activation of several molybdoenzymes in *Escherichia coli* K12. *Biochim Biophys Acta - Gen
709 Subj* **798**: 216–225.
710
- 711 Glaser, J.H., and DeMoss, J.A. (1971) Phenotypic Restoration by Molybdate of Nitrate
712 Reductase Activity in *chlD* Mutants of *Escherichia coli*. *J Bacteriol* **108**: 854–860.
713
- 714 Goblirsch, B.R., Streit, B.R., DuBois, J.L., and Wilmot, C.M. (2010) Structural features
715 promoting dioxygen production by *Dechloromonas aromatica* chlorite dismutase. *JBIC J
716 Biol Inorg Chem* **15**: 879–888.
717
- 718 Hajj, S. El, Henry, C., Andrieu, C., Vergnes, A., Loiseau, L., Brasseur, G., *et al.* (2022) HprSR Is
719 a Reactive Chlorine Species-Sensing, Two-Component System in *Escherichia coli*. *J
720 Bacteriol* **204**.
721
- 722 Henry, C., Loiseau, L., Vergnes, A., Vertommen, D., Mérida-Floriano, A., Chitteni-Pattu, S., *et
723 al.* (2021) Redox controls reca protein activity via reversible oxidation of its methionine
724 residues. *Elife* **10**: 1–59.
725
- 726 Imlay, J. a (2015) Diagnosing oxidative stress in bacteria: not as easy as you might think.
727 *Curr Opin Microbiol* **24**: 124–131
728 <http://linkinghub.elsevier.com/retrieve/pii/S1369527415000053>.
729
- 730 Imlay, J.A. (2013) The molecular mechanisms and physiological consequences of oxidative

- 731 stress: lessons from a model bacterium. *Nat Rev Microbiol* **11**: 443–454.
- 732
- 733 Imlay, J.A. (2019) Where in the world do bacteria experience oxidative stress? *Environ*
734 *Microbiol* **21**: 521–530.
- 735
- 736 Kiley, P.J., and Beinert, H. (1998) Oxygen sensing by the global regulator, FNR: the role of
737 the iron-sulfur cluster. *FEMS Microbiol Rev* **22**: 341–352.
- 738
- 739 Kim, G., Weiss, S.J., and Levine, R.L. (2014) Methionine oxidation and reduction in proteins.
740 *Biochim Biophys Acta - Gen Subj* **1840**: 901–905
741 <http://dx.doi.org/10.1016/j.bbagen.2013.04.038>.
- 742
- 743 Lee, Y., Do, H.L., Chang, W.K., Ah, Y.L., Jang, M., Cho, S., *et al.* (2005) Transthyretin-related
744 proteins function to facilitate the hydrolysis of 5-hydroxyisourate, the end product of the
745 uricase reaction. *FEBS Lett* **579**: 4769–4774.
- 746
- 747 Loschi, L., Brokx, S.J., Hills, T.L., Zhang, G., Bertero, M.G., Lovering, A.L., *et al.* (2004)
748 Structural and biochemical identification of a novel bacterial oxidoreductase. *J Biol Chem*
749 **279**: 50391–400 <http://www.ncbi.nlm.nih.gov/pubmed/15355966>.
- 750
- 751 Lowther, W.T., Weissbach, H., Etienne, F., Brot, N., and Matthews, B.W. (2002) The
752 mirrored methionine sulfoxide reductases of *Neisseria gonorrhoeae* pilB. *Nat Struct Biol* .
- 753
- 754 Magalon, A., and Mendel, R.R. (2015) Biosynthesis and Insertion of the Molybdenum
755 Cofactor. *EcoSal Plus* **6**.
- 756
- 757 Mandin, P., and Gottesman, S. (2009) A genetic approach for finding small RNAs regulators
758 of genes of interest identifies RybC as regulating the DpiA/DpiB two-component system.
759 *Mol Microbiol* **72**: 551–565.
- 760
- 761 Melnyk, R.A., Youngblut, M.D., Clark, I.C., Carlson, H.K., Wetmore, K.M., Price, M.N., *et al.*
762 (2015) Novel Mechanism for Scavenging of Hypochlorite Involving a Periplasmic
763 Methionine-Rich Peptide and Methionine Sulfoxide Reductase. *MBio* **6**: 1–8.

- 764 Merdanovic, M., Clausen, T., Kaiser, M., Huber, R., and Ehrmann, M. (2011) Protein quality
765 control in the bacterial periplasm. *Annu Rev Microbiol* **65**: 149–68
766 <http://www.ncbi.nlm.nih.gov/pubmed/21639788>.
767
- 768 Miller, J.H. (1992) *A short course in bacterial genetics: a laboratory manual and handbook*
769 *for Escherichia coli and related bacteria*. Cold Spring Harbor Laboratory Press, Cold Spring
770 Harbor, NY, .
771
- 772 Myers, K.S., Yan, H., Ong, I.M., Chung, D., Liang, K., Tran, F., *et al.* (2013) Genome-scale
773 Analysis of Escherichia coli FNR Reveals Complex Features of Transcription Factor
774 Binding. *PLoS Genet* **9**: e1003565.
775
- 776 Saleh, M., Bartual, S.G., Abdullah, M.R., Jensch, I., Asmat, T.M., Petruschka, L., *et al.* (2013)
777 Molecular architecture of streptococcus pneumoniae surface thioredoxin-fold lipoproteins
778 crucial for extracellular oxidative stress resistance and maintenance of virulence. *EMBO*
779 *Mol Med* **5**: 1852–1870.
780
- 781 Schramm, F.D., Schroeder, K., and Jonas, K. (2020) Protein aggregation in bacteria. *FEMS*
782 *Microbiol Rev* **026**: 54–72 <https://orcid.org/0000-0002-6271-4530>.
783
- 784 Sheng, Y., Abreu, I.A., Cabelli, D.E., Maroney, M.J., Miller, A.-F., Teixeira, M., and Valentine, J.S.
785 (2014) Superoxide Dismutases and Superoxide Reductases. *Chem Rev* **114**: 3854–3918.
786
- 787 Skaar, E.P., Tobiason, D.M., Quick, J., Judd, R.C., Weissbach, H., Etienne, F., *et al.* (2002) The
788 outer membrane localization of the Neisseria gonorrhoeae MsrA/B is involved in survival
789 against reactive oxygen species. *Proc Natl Acad Sci U S A* **99**: 10108–13
790 [http://www.pubmedcentral.nih.gov/articlerender.fcgi?artid=126632&tool=pmcentrez&re](http://www.pubmedcentral.nih.gov/articlerender.fcgi?artid=126632&tool=pmcentrez&rendertype=abstract)
791 [ndertype=abstract](http://www.pubmedcentral.nih.gov/articlerender.fcgi?artid=126632&tool=pmcentrez&rendertype=abstract).
792
- 793 Spiro, S. (1994) The FNR family of transcriptional regulators. *Antonie Van Leeuwenhoek* **66**:
794 23–36.
795
- 796 Stewart, V. (1988) Nitrate respiration in relation to facultative metabolism in

797 enterobacteria. *Microbiol Rev* **52**: 190–232.

798

799 Vaughan, M. (1997) Oxidative Modification of Macromolecules Minireview Series. *J Biol*
800 *Chem* **272**: 18513.

801

802 Wang, O., and Coates, J. (2017) Biotechnological Applications of Microbial (Per)chlorate
803 Reduction. *Microorganisms* **5**: 76.

804

805 Warne, S.R., Varley, J.M., Boulnois, G.J., and Norton, M.G. (1990) Identification and
806 Characterization of a Gene that Controls Colony Morphology and Auto-Aggregation in
807 *Escherichia Coli* K12. *J Gen Microbiol* **136**: 455–462

808 [https://www.microbiologyresearch.org/content/journal/micro/10.1099/00221287-136-](https://www.microbiologyresearch.org/content/journal/micro/10.1099/00221287-136-3-455)
809 [3-455.](https://www.microbiologyresearch.org/content/journal/micro/10.1099/00221287-136-3-455)

810

811 Winterbourn, C.C., and Kettle, A.J. (2013) Redox Reactions and Microbial Killing in the
812 Neutrophil Phagosome. *Antioxid Redox Signal* **18**: 642–660.

813

814 Zupok, A., Iobbi-Nivol, C., Méjean, V., and Leimkühler, S. (2019) The regulation of Moco
815 biosynthesis and molybdoenzyme gene expression by molybdenum and iron in bacteria.
816 *Metallomics* **11**: 1602–1624.

817

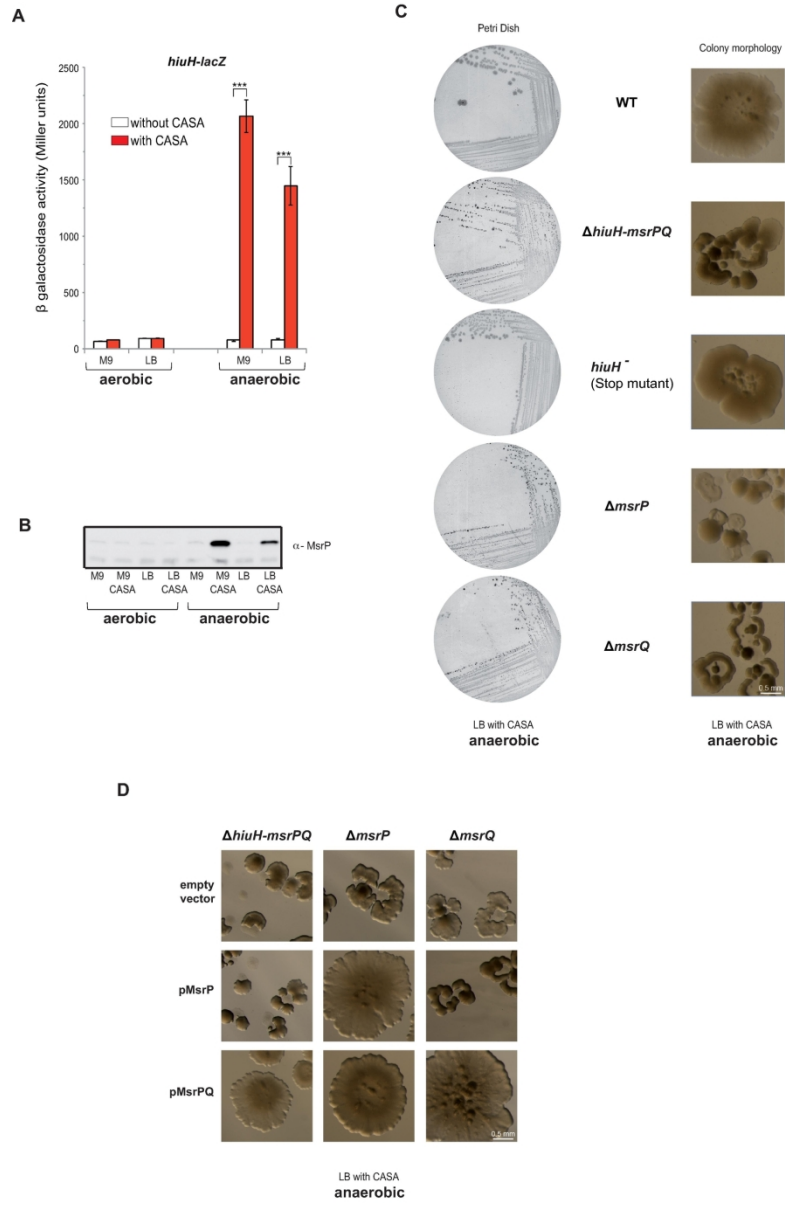


figure 1

151x233mm (300 x 300 DPI)

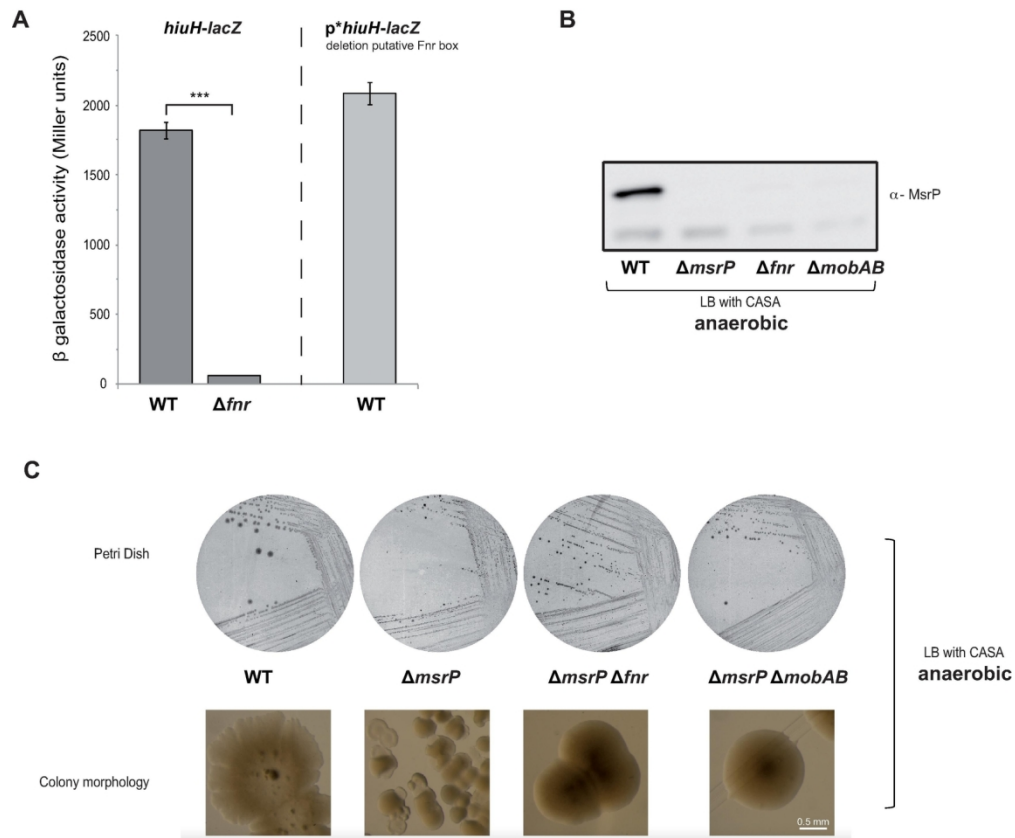


figure 2

146x121mm (300 x 300 DPI)

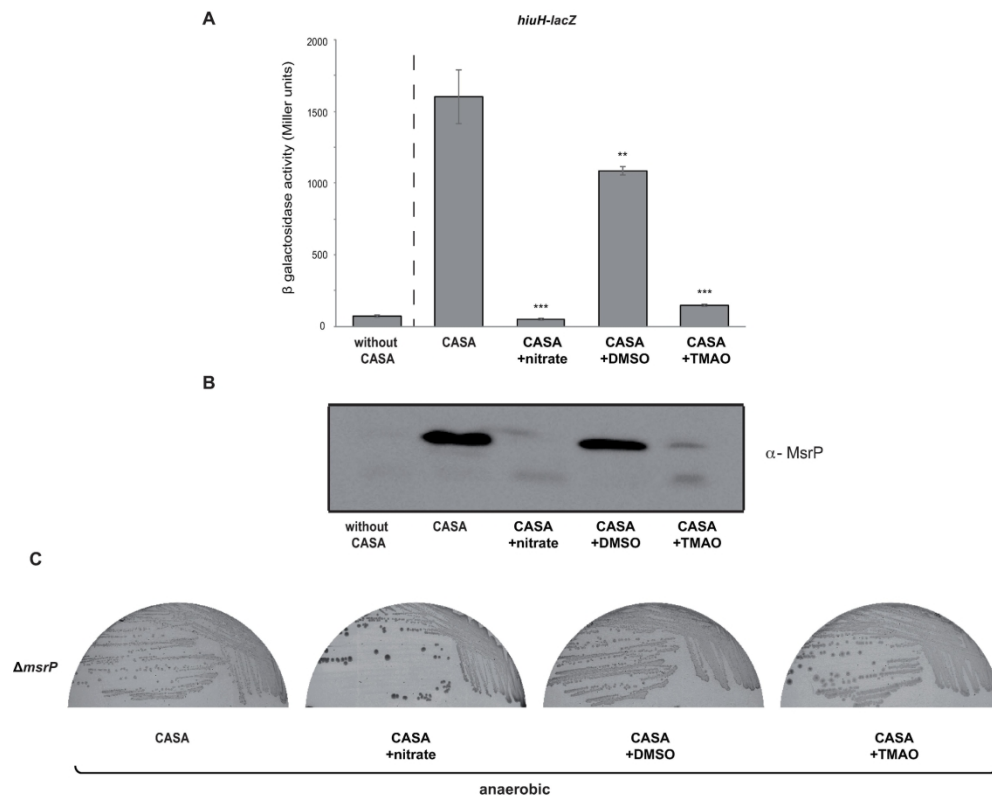


figure 3

192x152mm (300 x 300 DPI)

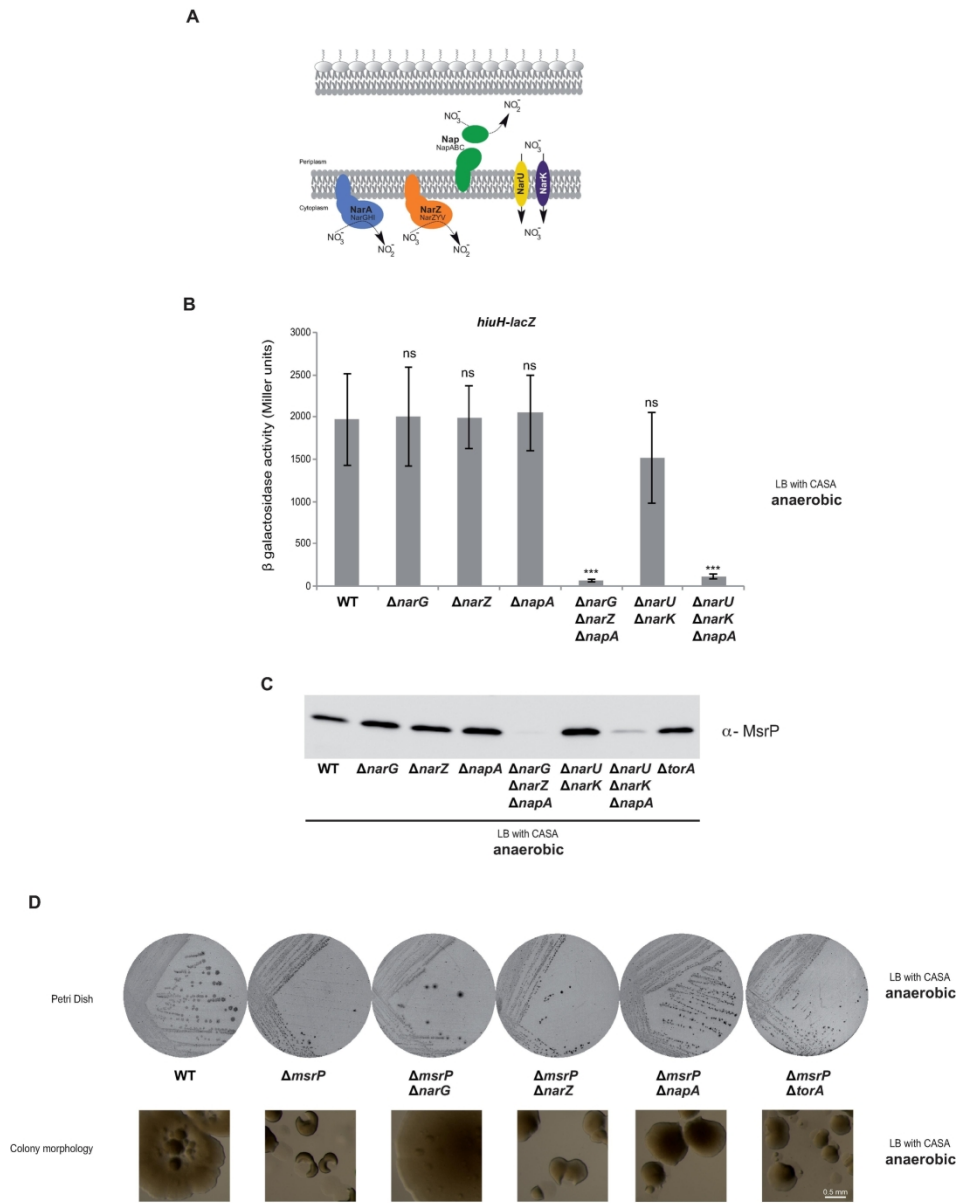


figure 4

183x232mm (300 x 300 DPI)

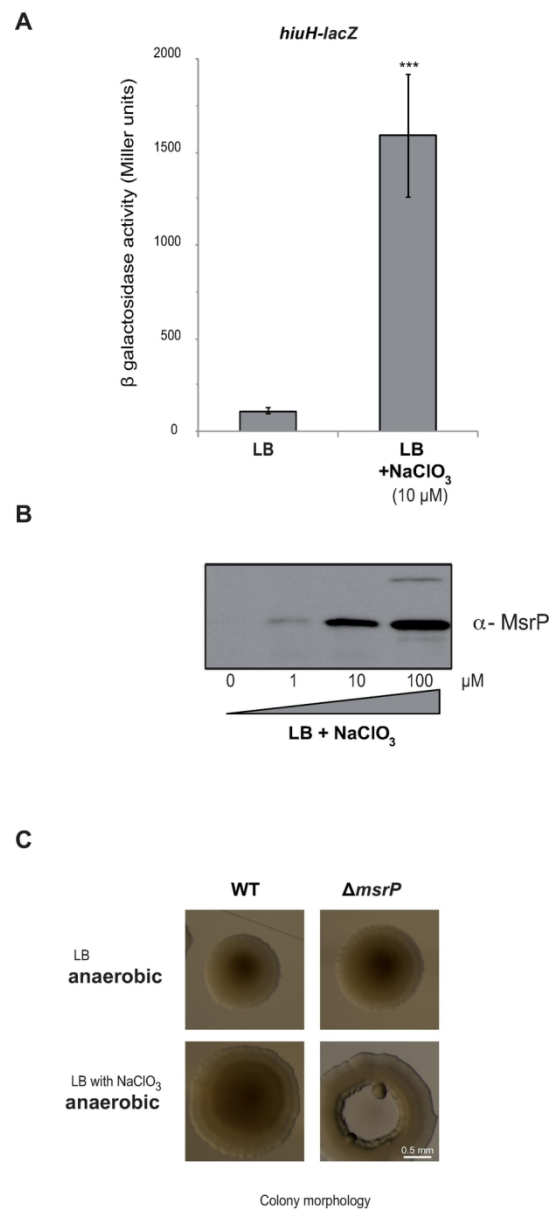


figure 5

77x174mm (300 x 300 DPI)

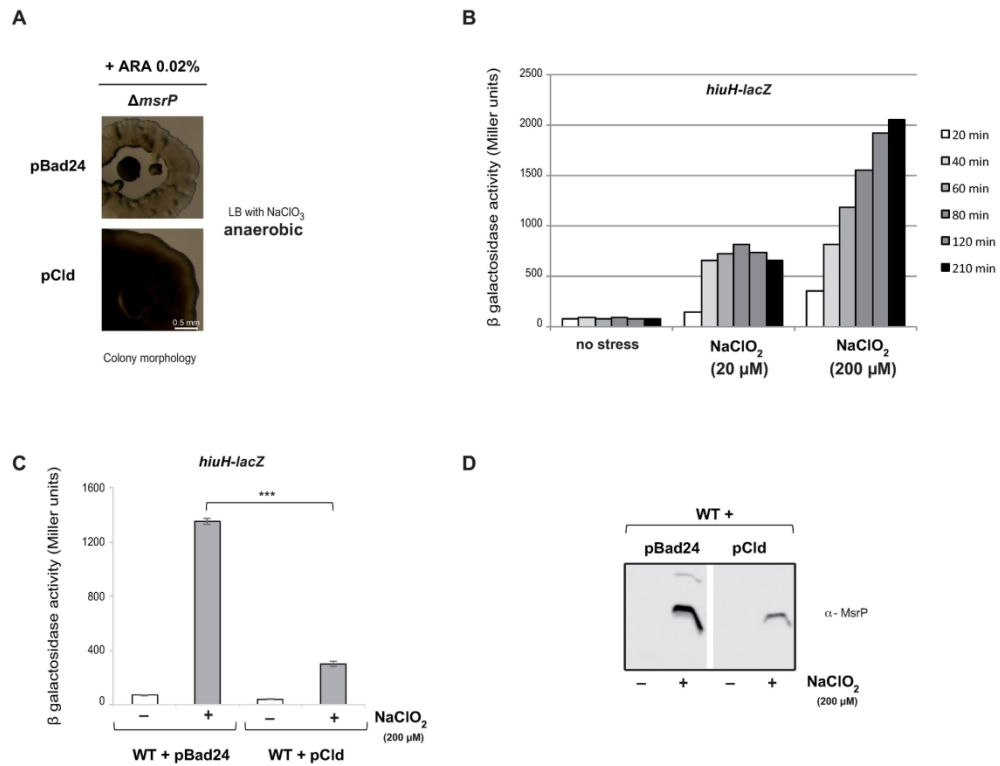


figure 6

173x131mm (300 x 300 DPI)

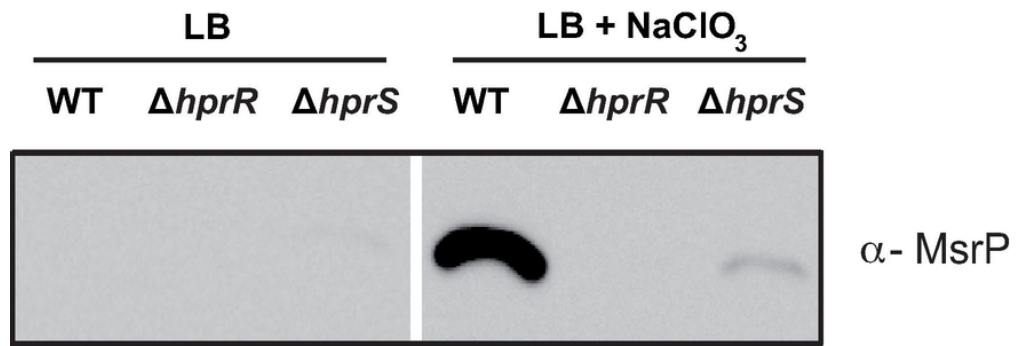


figure 7

73x25mm (300 x 300 DPI)

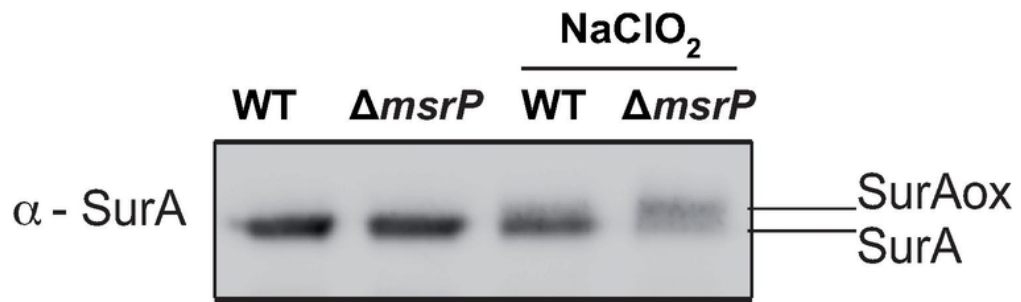


figure 8

64x18mm (300 x 300 DPI)

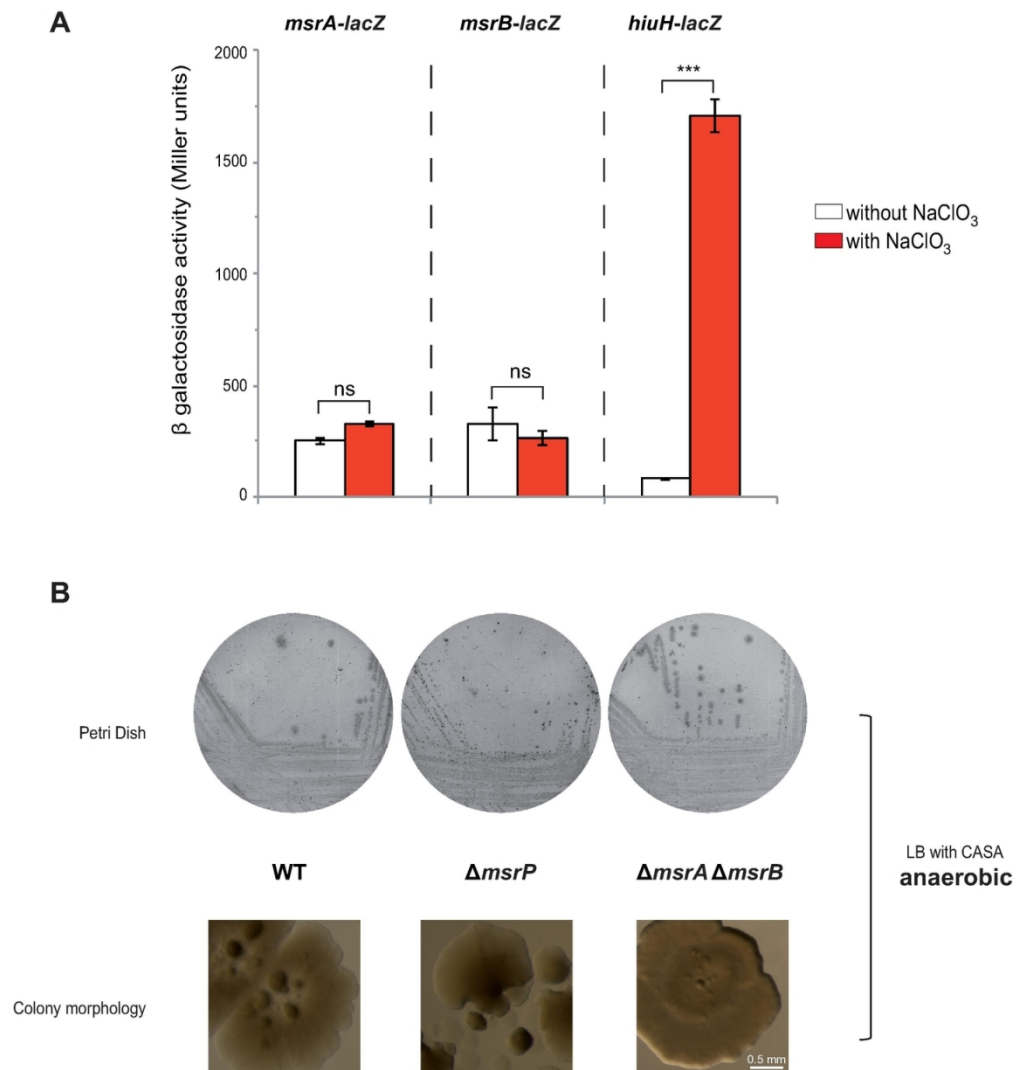
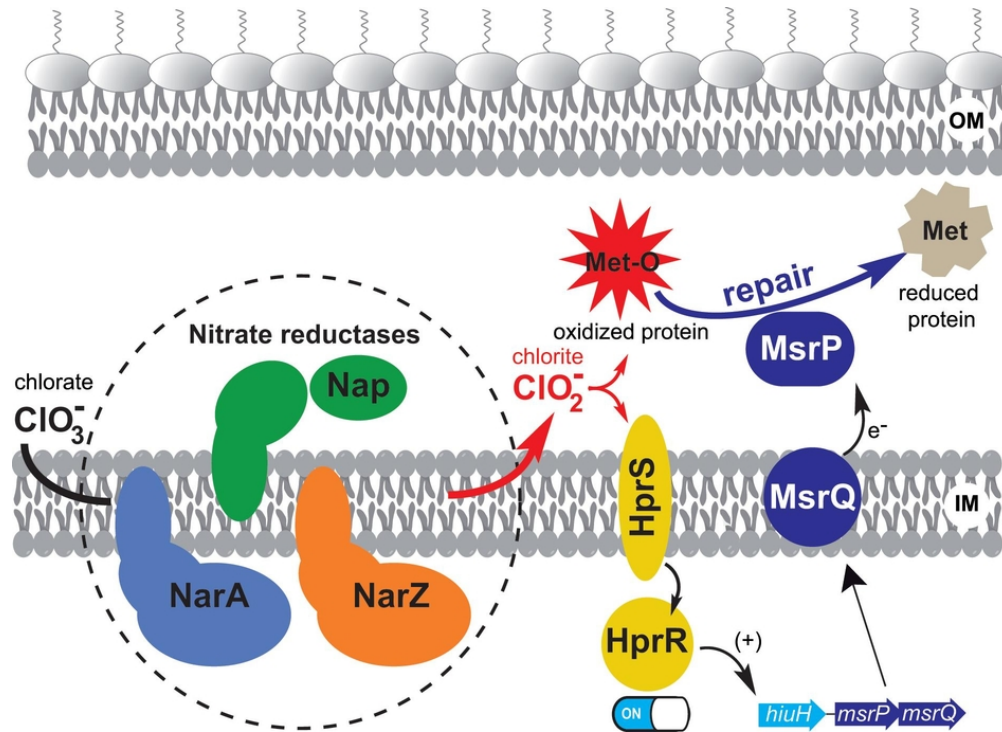


figure 9

121x129mm (300 x 300 DPI)



In anaerobic condition, reduction of chlorate (ClO_3^-) to the toxic oxidizing agent chlorite (ClO_2^-) by the three nitrate reductases (NarA, NarZ and Nap) led to methionine oxidation of periplasmic proteins. In response to this stress the *E. coli* HprSR two-component system was activated, leading to over-production of the periplasmic methionine sulfoxide reductase (MsrPQ) and the repair of the oxidized proteins.

80x57mm (300 x 300 DPI)

Summary graphical abstract :

In anaerobic condition, reduction of chlorate (ClO_3^-) to the toxic oxidizing agent chlorite (ClO_2^-) by the three nitrate reductases (NarA, NarZ and Nap) led to methionine oxidation of periplasmic proteins. In response to this stress the *E. coli* HprSR two-component system was activated, leading to over-production of the periplasmic methionine sulfoxide reductase (MsrPQ) and the repair of the oxidized proteins.

For Peer Review